Carbohydrate Polymers 85 (2011) 845–853

Contents lists available at ScienceDirect

Carbohydrate Polymers

journal homepage: www.elsevier.com/locate/carbpol

Formation and properties of a novel complex composed of an amylose-grafted chitosan derivative and single-walled carbon nanotubes

Liqun Yang*, Bin Yang, Di Zeng, Dan Wang, Yu Wang, Li-Ming Zhang

Institute of Polymer Science, School of Chemistry and Chemical Engineering, BME Center, State Key Laboratory of Optoelectronic Materials and Technologies, DSAPM Lab and PCFM Lab, Sun Yat-Sen University, Guangzhou 510275, China

ARTICLE INFO

Article history:
Received 18 January 2011
Received in revised form 1 March 2011
Accepted 4 April 2011
Available online 9 April 2011

Keywords:
Amylose
Chitosan
Enzymatic polymerization
Complex
Single-walled carbon nanotube

ABSTRACT

The water-soluble chitosan derivative grafted with short amylose chains (Chit-Amy-III) was synthesized through the phosphorylase-catalyzed enzymatic polymerization, following that the chitosan was grafted with maltoheptaose residues by reductive amination. The chemical structures were characterized by FTIR, ^{1}H NMR, Raman, XRD and static light scattering analyses. The results indicated that the amylose chains were conjugated with the chitosan backbone through the reductive Shiff base bonds (–CH–NH–), and the polymerization degree of the grafted amylose chains was about 25. The dispersion stability of single-walled carbon nanotubes (SWNTs) in water was improved through the complexation of Chit-Amy-III derivatives with SWNTs. Raman, XRD and TEM analyses confirmed that the resultant Chit-Amy-SWNTs complex was formed by the wrapping of the Chit-Amy-III derivative around the SWNTs. The results of electrochemical analysis indicated that the Chit-Amy-SWNTs complex modified electrode displayed excellent electron conductivity and electrocatalytic activity on H_2O_2.

1. Introduction

Amylose is a naturally occurring linear polysaccharide consisting of α-1,4-D-glucose units, which occurs in starch granules together with amylopectin. As a result of hydrophobic interactions between guest molecules and the cylindrical cavity inside amylose helix (Star, Steuerman, Heath, & Stoddart, 2002), amylose is well-known to form inclusion complexes with a wide range of ligand molecules, such as single-walled carbon nanotubes (SWNTs) (Fu, Meng, Lu, Zhang, & Gao, 2007; Star et al., 2002; Yang et al., 2008), genistein (Cohen, Orlova, Kovalev, Ungar, & Shimoni, 2008), lactones (Heinemann, Escher, & Conde-Petit, 2003), linoleic acid (Lalush, Bar, Zakaria, Eichler, & Shimoni, 2005), lipid (Gelders, Goesaert, & Delcour, 2005), and iodine (Cesaro, Benegas, & Ripoll, 1986). However, the extended applications of these complexes are usually limited due to the lack of water-solubility and biocompatibility.

Amylose aggregates in aqueous solution and precipitates on account of the strong intra- and inter-molecular hydrogen bonds between amylose molecules. The aggregation rate is dependent on the chain lengths of amylose (Gidley & Bulpin, 1989). It was found that amylose was more soluble in aqueous solution at the polymerization degree less than 50 because of the low aggregation rate (Gidley & Bulpin, 1989; Pfannemuller, Mayerhofer, & Schulz, 1971). On the other hand, chitosan, a deacetylated derivative of chitin, has been investigated for a broad range of applications in biomaterials owing to the excellent compatibility with cells, proteins and nucleic acids (Bhattarai, Edmondson, Veiseh, Matsen, & Zhang, 2005), such as in gene delivery systems (Lu et al., 2009; Strand, Issa, Christensen, Varum, & Artursson, 2008), tissue engineering (Cruz et al., 2008; Martino, Sittinger, & Risbud, 2005) and biosensors (Najeeb, Chang, Lee, Lee, & Kim, 2011; Zhang, Smith, & Gorski, 2004), and as carriers for drug delivery (Kato, Onishi, & Machida, 2004; Yu, Li, Qiu, & Jin, 2008). Therefore, the water-solubility and biocompatibility of the amylose complexes are anticipated to be improved by synthesis of water-soluble chitosan derivatives grafted with short amylose chains.

SWNTs are single sheets of graphite rolled into seamless cylinders with a diameter of about 1 nm and a length of several micrometers, of which the surface and channel are nonpolar and hydrophobic (Star et al., 2002). Since their discovery, SWNTs have been considered as a potential new material because of their excellent electrical and mechanical properties. For example, the SWNTs modified electrodes have attracted much attention in biosensors (Ding, Wang, & Lei, 2010; Gooding et al., 2003; Shi et al., 2009). However, the poor dispersion stability of SWNTs in solution has greatly limited their applications. In this work, the water-soluble chitosan derivatives grafted with short amylose chains were synthesized through the phosphorylase-catalyzed enzymatic polymerization, following that the chitosan was grafted with maltoheptaose residues by reductive amination with the aid of the previous works (Izawa, Nawaji, Kaneko, & Kadokawa,

* Corresponding author. Tel.: +86 20 84110934; fax: +86 20 84112245.
E-mail address: yanglq@mail.sysu.edu.cn (L. Yang).

0144-8617/$ – see front matter © 2011 Elsevier Ltd. All rights reserved.
doi:10.1016/j.carbpol.2011.04.005

2009; Kaneko, Matsuda, & Kadokawa, 2007; Matsuda, Kaneko, & Kadokawa, 2007; Omagari, Matsuda, Kaneko, & Kadokawa, 2009; Omagari, Kaneko, & Kadokawa, 2010). The complex of the amylose-grafted chitosan derivatives with SWNTs were prepared to improve the dispersion stability in aqueous solution and biocompatibility of SWNTs. The electrochemical property of the complex based electrode was investigated for future application in the biosensor field.

2. Materials and methods

2.1. Materials

Chitosan, with a deacetylation degree above 95%, was purchased from Shanghai Bio Life Science & Technology Co., Ltd. (Shanghai, China). Chitosan was degraded through the H_2O_2 oxidation method according to the literature (Qin, Du, & Xiao, 2002). Briefly, chitosan (1.0 g) was dissolved in 80 mL of 0.1 mol/L aqueous acetic acid. After 0.2 mL of 30% H_2O_2 solution was added, the hydrolysis was carried out by stirring at 45 °C for 4 h. The reaction mixture was then treated with ethanol/dilute ammonia liquor (v/v = 7/3) for adjustment of the pH value to 9 and precipitation of the degraded chitosan (Chit-deg). The precipitate was washed with distilled water and dried in vacuum at 45 °C for 4 h to provide the solid Chit-deg. The weight average molecular weights (M_w) of chitosan and the Chit-deg product were determined to be 4.5×10^5 g/mol and 4.0×10^4 g/mol by the viscosity method, using the Mark–Houwink equation in the mixture aqueous solutions of sodium acetate (0.1 mol/L) and acetic acid (0.2 mol/L) (1/1, v/v, pH ≈ 3) at 30 °C (Wang, Bo, & Qin, 1991): $[\eta] = 6.589 \times 10^{-3} M_w^{0.88}$.

β-Cyclodextrin was bought from Fluka company (Buchs, Switzerland). Maltoheptaose was synthesized by acid catalyzed cleavages of one glycosidic bond of β-cyclodextrin (Braunmuhl, Jonas, & Stadler, 1995; Loos, Braunmuh, & Stadler, 1997). α-D-Glucose 1-phosphate (Glc-1-P) was purchased from Aldrich company (Steinheim, Germany). The purified SWNTs, with purity above 90%, length of about 5–30 μm, and diameter of 1–2 nm, were bought from Chengdu Organic Chemistry Co., Ltd, Chinese Academy of Sciences. Potato phosphorylase was isolated and its activity was determined by phosphate analysis to be 16.0 Unit/mL according to our previously published work (Yang et al., 2008). All other reagents were analytical grade and used as received.

2.2. Synthesis of maltoheptaose-grafted chitosan (Chit-Glc7) derivatives

The reaction was carried out as follows according to Table S1 in Supplementary Data: the Chit-deg (1.000 g, 6.2 mmol amino glucose units) was dissolved in 22 mL of 0.1 mol/L aqueous acetic acid. Then, the different amounts of maltoheptaose and sodium cyanotrihydroborate ($NaBH_3CN$) were added with vigorous stirring at room temperature. After the reaction was allowed to proceed at room temperature for 5 days, the reaction mixture was neutralized with 5% (w/v) aqueous Na_2CO_3 solution to yield the Chit-Glc7 derivatives.

For water-insoluble Chit-Glc7-I, -II and -III products, the reaction mixtures were centrifuged (15,000 rpm, 15 min). The resultant products were then purified twice by dissolving the precipitate in 10 mL of 0.1 mol/L aqueous acetic acid, neutralizing with 5% (w/v) aqueous Na_2CO_3 solution and centrifuging at 15,000 rpm for 15 min. The resultant precipitation was lyophilized. For the water-soluble Chit-Glc7-IV, the resulted aqueous solution was dialyzed against distilled water for 3 days in a dialysis bag (molecular weight cutoff 5000) to remove unreacted maltoheptaose, and lyophilized to provide the pure product.

2.3. Synthesis of the amylose-grafted chitosan (Chit-Amy) derivatives

As illustrated in Table S2 in Supplementary Data, the water-soluble Chit-Glc7-IV (0.1000 g, 0.14 mmol maltoheptaose grafted amino glucose units) was dissolved in 20 mL of sodium citrate buffer (pH 6.2). Then, 3 mL of phosphorylase solution and the different amounts of Glc-1-P were added. The reaction was performed in a nitrogen atmosphere by stirring at 40 °C for 3 h. The water-insoluble Chit-Amy-I derivative was isolated by centrifugation (4000 rpm, 10 min) and lyophilized. For the suspension and water-soluble amylose-grafted chitosan derivatives (Chit-Amy-II and -III), the enzymatic amylose synthesis was stopped by boiling for 10 min. Denatured phosphorylase was removed by centrifuging at 3500 rpm for 10 min. The supernatant was dialyzed against distilled water for 3 days following the above mentioned method, and lyophilized to yield the products.

2.4. Preparation of the complex of Chit-Amy-III derivative and SWNTs (Chit-Amy-SWNTs)

After Chit-Amy-III (50 mg) was dissolved in 10 mL of distilled water, SWNTs (2 mg) were added with vigorous stirring. The mixture solution was then discontinuously ultrasonicated at room temperature for 1 h (1 s on and 1 s off), using VCX 130 Ultrasonic Processor (Sonics & Materials Inc., Virginia, USA). The resulting black supernatant containing SWNTs was separated after the solution was kept at 5 °C overnight to provide the Chit-Amy-SWNT complex.

2.5. Structural characterization

FTIR measurement was performed with an FTIR Analyzer (Nicolet/Nexus 670, Thermo Nicolet Corporation, Wisconsin, USA) at a resolution of 4 cm^{-1} using the KBr method. UV–vis measurement was performed on a UV–vis spectrophotometer (UV-3150, Shimadzu Corporation, Kyoto, Japan).

^1H NMR experiment was performed on an NMR Spectrometer (Mercury-Plus 300, Varian, Inc., California, USA) at 50 °C. The Chit-Glc7-IV derivative was dissolved in D_2O, and the Chit-Glc7-I, -II and -III derivatives were dissolved in DCl/D_2O (0.1 mol/L), respectively, to a final concentration of 20 mg/mL. ^1H NMR chemical shifts were referred to that of HDO at 4.50 ppm (Gottlieb, Kotlyar, & Nudelman, 1997).

The X-ray diffraction (XRD) measurements were performed at a scanning speed of $2\theta = 5°$/min using a DMAX 2200 VPC X-Ray diffractometer (Rigaku Co., Tokyo, Japan). The X-ray radiation Cu $K\alpha_1$ ($\lambda = 0.15418$ nm) was selected with a quartz monochromator.

Raman scattering studies were performed with a Laser Micro-Raman Spectrometer (Renishaw inVia, Britain) at 1 cm^{-1} resolution, using a laser excitation wavelength at 785 nm with 300 mW and an argon ion excitation wavelength at 514.5 nm with 20 mW. An aqueous sample of the complex of Chit-Amy-III derivative and SWNTs was filled in a glass capillary tube and then was measured. Other solid samples were measured on a clean glass microscope slide.

In transmission electron microscopy (TEM) experiment, an aqueous sample of the complex of Chit-Amy-III derivative and SWNTs was dropped on a 200-mesh copper grid deposited by carbon and dried in the air. The high-resolution transmission electron microscopic (HR TEM) images were obtained on a transmission electron microscope (JEOL JEM-2010HR, JEOL Ltd., Japan).

2.6. Static light scattering analysis

The static light scattering measurements were performed with a dynamic/static laser scattering system (BI-200SM, Brookhaven Instruments Corporation, New York, USA) at 25 °C with the scattering angles varied from 30° to 150°. The sample solutions were prepared by dissolving the derivatives of Chit-Glc7-IV and Chit-Amy-III in 0.1 mol/L aqueous citric acid/trisodium citrate buffer solution and DMSO, and then filtering through membrane filters (nominal pore sized 0.45 μm), respectively. The dn/dc values were determined to be 0.1257 and 0.0967 mL/g for them, respectively.

The M_w value was determined by the Zimm method based on the Rayleigh–Gans–Debye theory for light scattering through Eq. (1).

$$\frac{Kc}{R_\theta} = \frac{1}{M_w}\left[1 + \frac{16\pi^2 n^2}{3\lambda^2} R_g^2 \sin^2\left(\frac{\theta}{2}\right)\right] + 2A_2 c \quad (1)$$

where the optical constant $K = [4\pi^2 n^2 (dn/dc)^2]/(N_A \lambda^4)$; n is the refraction index of solvent and solution; θ is the observation angle; λ is the wavelength in vacuum of the laser, N_A is Avogadro's number and c is the concentration of the polymer solution; R_g is the radius of gyration; and A_2 is the second virial coefficient. The Rayleigh ratio, $R_\theta = (I_\theta r^2/I_0)$, I_0 and I_θ are the intensity of the incident light and the scattered light, r is the distance from the light source to the measuring point. A plot of (Kc/R_θ) against $[\sin^2(\theta/2) + kc]$ can be used to determine the molecular parameters (where k is an arbitrary constant). By extrapolating the data to zero angles and concentrations, the intercept of both extrapolated lines to zero angles and zero concentrations yields M_w.

2.7. Measurements of electrochemical property of the glassy carbon electrode modified with the Chit-Amy-SWNTs complex

The CHI 104 glassy carbon (GC) disc electrode (3 mm diameter) was purchased from CH Instruments, Inc. (Electrochemical Instrumentation, Texas, USA). Before used, the GC electrode was wet polished on a polishing cloth with particles of Al_2O_3 (0.3 and 0.05 μm diameter), and then was soaked in of ethanol and the distilled water for 10 min, respectively. 20 μL of the Chit-Amy or Chit-Amy-SWNTs solutions were sequentially dropped on to the electrode surface. The modified electrodes were dried in the air.

Electrochemical measurements were performed on a CHI 660A Electrochemical Work Station (Shanghai Chenhua Instrument Co., Shanghai, China) with a three-electrode system in 50 mL of phosphate buffer solution (pH 7.0). The modified or naked GC electrodes, platinum wire and saturated calomel electrode (SCE) were used as working, auxiliary and reference electrodes, respectively. Cyclic voltammetric experiments were carried out by applying a potential from −0.6 to 1 V at different scan speeds. The current responses of the working electrode were measured at an applied potential of 1.0 V in the phosphate buffer solutions (pH 7.0), to which was added a series of H_2O_2 solutions (0.001–8.8 mol/L), respectively. Magnetic stirring provided the convective transport during the measurements.

3. Results and discussion

3.1. Synthesis and characterization of the water-soluble Chit-Glc7 derivatives

The Chit-Glc7 derivatives were synthesized through the reductive amination between the hemiacetal groups of maltoheptaose and the primary amino groups of the Chit-deg in aqueous acetic acid (Scheme S1 in Supplementary Data). The FTIR spectrum of the Chit-deg shows an absorption at 1605 cm^{-1} (Fig. 1a), which is attributed

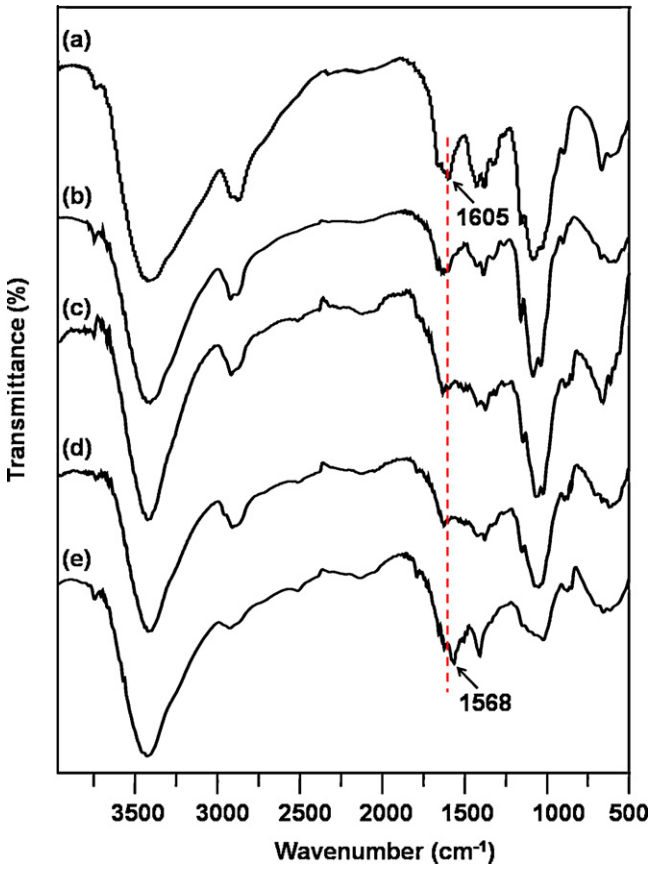

Fig. 1. FTIR spectra of (a) the Chit-deg, (b) Chit-Glc7-I, (c) Chit-Glc7-II, (d) Chit-Glc7-III and (e) Chit-Glc7-IV.

to the primary amino groups of the Chit-deg (Wang, 2008; Wu, 1994). This absorption decreases with increasing amounts of added maltoheptaose for the Chit-Glc7 derivatives (Fig. 1b–e), indicating that more and more primary amino groups of the Chit-deg has reacted with maltoheptaose. In FTIR spectrum of Chit-Glc7-IV derivative (Fig. 1e), the obvious absorption at 1568 cm^{-1}, assigned to the secondary amino groups, further proves that maltoheptaose residues were conjugated with the chitosan backbones through the reductive Shiff base bonds (–CH–NH–) (Wu, 1994).

The ^1H NMR spectra of the Chit-Glc7 derivatives are shown in Fig. 2. The signals in the range of 3.5–4.0 ppm are assigned to the H2–H6 of the chitosan main chains and the maltoheptaose residues. In the range from 4.7 to 5.5 ppm, several resonance peaks due to the anomeric protons appeared. For Chit-Glc7-I, -II and -III derivatives dissolved in 0.1 mol/L DCl/D_2O, the signals at 5.32, 4.85 and 4.82 ppm are attributed to the H1 of maltoheptaose residues and chitosan backbones (Fig. 2a–c), respectively. These resonances of the Chit-Glc7-IV derivative shifted to 5.35 and 5.08 ppm using D_2O as a solvent (Fig. 2d). The results further confirm that maltoheptaose residues were conjugated with the Chit-deg backbone through covalent bonds, which are in good agreement with the previous works (Matsuda et al., 2007). In addition, with increasing the added amount of maltoheptaose, an increasing in the intensity of H1 resonances at 5.32 and 5.35 ppm was observed, suggesting more and more maltoheptaose was conjugated with the chitosan chains. The grafting degree (DG) of maltoheptaose residues, defined as the average number of maltoheptaose residues (N_{Glc7}) grafted with per 100 amino glucose units on the chitosan main chains as shown in Eq. (2), was evaluated from integration of the H1 signals of maltoheptaose residues and chitosan backbones. As a result, the DG values of Chit-Glc7-I, II, -III and -IV derivatives were deter-

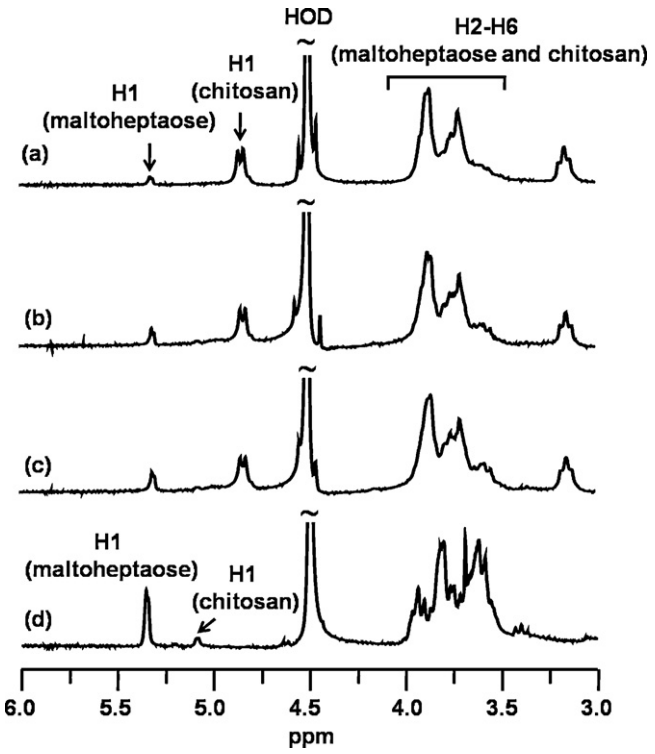

Fig. 2. ^{1}H NMR spectra of (a) Chit-Glc7-I, (b) Chit-Glc7-II and (c) Chit-Glc7-III in DCl/D_2O (0.1 mol/L), and (d) Chit-Glc7-IV in D_2O.

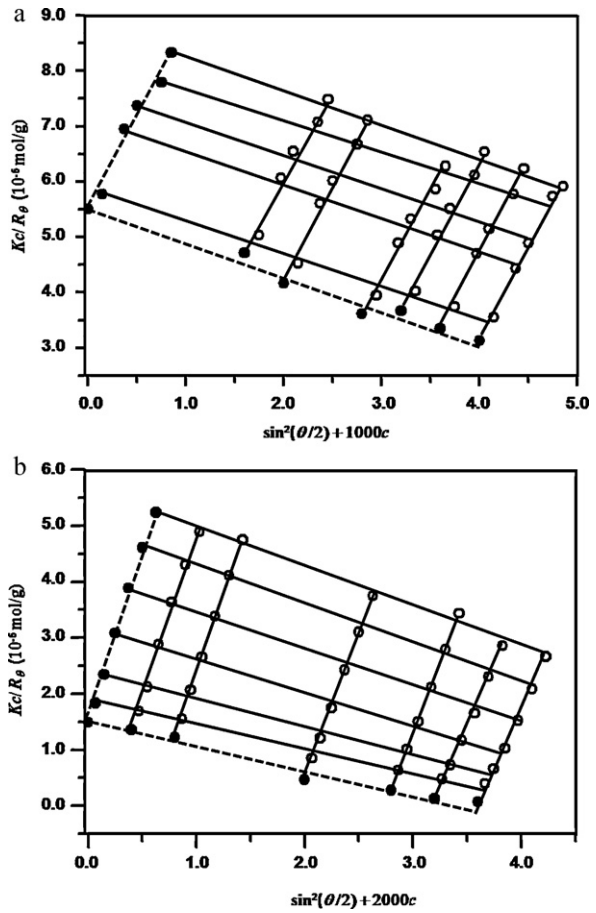

Fig. 3. Zimm plots of the chitosan derivatives: (a) Chit-Glc7-IV in 0.1 mol/L aqueous citric acid/trisodium citrate buffer solution and (b) Chit-Amy-III in DMSO.

mined to be 3.2, 4.6, 4.9 and 48% (Table S1 in Supplementary Data), respectively.

$$DG = \left(\frac{N_{Glc7}}{N_{Glc\text{-}NH2}}\right) \times 100\% \quad (2)$$

where $N_{Glc\text{-}NH2}$ is the number of amino glucose units on the chitosan main chains.

The M_w value of the water soluble Chit-Glc7-IV derivative was determined be 1.8×10^5 g/mol according to the Zimm plots of the Chit-Glc7-IV using static light scattering analysis (Fig. 3a). In consequence, the *DG* value was determined to be 49% (Table S1 in Supplementary Data), in agreement with the result of ^{1}H NMR analysis.

Chitosan is only soluble in an aqueous acidic solution, but insoluble in water or high pH solutions (Park, Cho, Chung, Kwon, & Jeong, 2003). The presence of rigid crystalline domains, formed by intra- and inter-molecular hydrogen bonding, is considered to be responsible for the poor water-solubility of chitosan (Nishimura, Kohgo, Kurita, & Kuzuhara, 1991). From the XRD pattern of the Chit-deg shown in Fig. 4a, it was found that the two diffraction peaks ($2\theta = 10.3^\circ$ and 19.7°) were derived from the crystalline structure of chitosan (Wang, 2008). However, the Chit-Glc7-IV derivative was well dissolved in water and became a transparent aqueous solution. This indicated that the water-solubility of chitosan was improved by grafting with maltoheptaose residues. Compared with the XRD pattern of the Chit-deg shown (Fig. 4a), the crystalline peaks of chitosan was eliminated and an amorphous peak ($2\theta = 20.0^\circ$) appeared in the XRD patterns of the Chit-Glc7-IV (Fig. 4b). It may give evidence that the crystalline structure of chitosan was destroyed by the grafted maltoheptaose residues, resulting in an excellent water-solubility of the Chit-Glc7-IV derivative.

3.2. Synthesis and characterization of the water-soluble Chit-Amy derivatives

In order to achieve the water-soluble Chit-Amy derivatives further, the phosphorylase-catalyzed enzymatic polymerization was performed based on the water-soluble Chit-Glc7-IV derivative (Scheme S1 in Supplementary Data). The polymerization was initiated from a primer of maltoheptaose and proceeds from Glc-1-P as a monomer catalyzed by potato phosphorylase, where a glucose residue was transferred from Glc-1-P to the non-reducing terminus of α-glucan chain, releasing inorganic phosphate (HPO_4^{2-}, Pi) (Yang et al., 2008). This process is similar to active anionic polymerization (Ziegast & Pfannemuller, 1987), that is, the polymerization degree (*PD*) of amylose residues could be controlled. Considering that the amylose was much more soluble in aqueous solution at the *PD* value less than 50 (Gidley & Bulpin, 1989; Pfannemuller et al., 1971), the Chit-Amy derivatives grafted with short amylose residues were thus synthesized by controlling the added amount of Glc-1-P (Table S2 in Supplementary Data).

As a result, the water solubility of the Chit-Amy derivatives was improved (Table S2 in Supplementary Data). The Chit-Amy-III derivative was well soluble in distilled water, of which M_w value was determined to be 6.7×10^5 g/mol according to the Zimm plots of in Fig. 3b. It was found that the M_w of the Chit-Amy-III was larger than that of the Chit-Glc7-IV, suggesting that the grafts of the Chit-Amy-III were longer than those of the Chit-Glc7-IV. The *PD* value of grafted amylose residues of the Chit-Amy was calculated to be 25

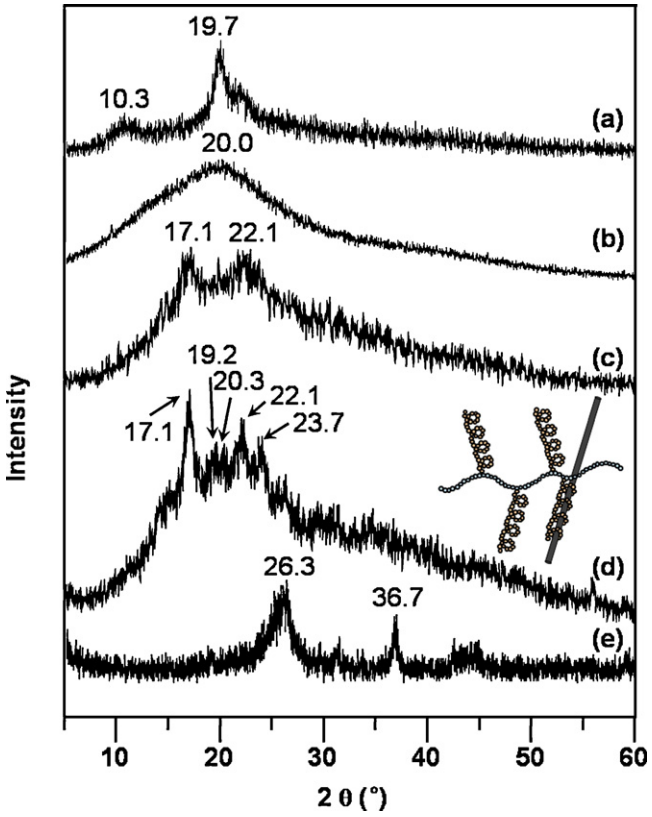

Fig. 4. XRD patterns of (a) Chit-deg, (b) Chit-Glc7-IV, (c) Chit-Amy-III, (d) Chit-Amy-SWNTs complex and (e) SWNTs (insert: proposed scheme of inclusion structure of Chit-Amy-SWNTs complex).

through the following equation:

$$PD = \frac{[M_{w(\text{Chit-Amy-III})} - M_{w(\text{Chit-Glc7-IV})}]}{(162 \times N_{\text{Glc7}})} \quad (3)$$

where $M_{w(\text{Chit-Amy-III})}$ and $M_{w(\text{Chit-Glc7-IV})}$ are the M_w of the Chit-Amy-III and Chit-Glc7-III derivatives, respectively, 162 is the molecular weight of glucose unit on the grafted amylose residues, and N_{Glc7} is the number of maltohexaose grafts per Chit-Glc7-IV macromolecule, which is determined from Eq. (5) by combination of Eqs. (2) and (4).

$$M_{w(\text{Chit-Glc7-IV})} = 161 \times N_{\text{Glc-NH2}} + 1154 \times N_{\text{Glc7}} \quad (4)$$

$$N_{\text{Glc7}} = \frac{M_{w(\text{Chit-Glc7-IV})}}{[(161/DG) + 1154]} \quad (5)$$

where 161 and 1154 are the molecular weights of the amino glucose unit and the grafted maltohexaose unit, respectively.

Raman spectroscopy is suitable for characterizing α-D-glucosidic polysaccharides, such as amylose, amylopectin and dextran (Yang & Zhang, 2009). It has been reported that a strong Raman band of α-1,4-D helical amylose locates at 865 cm^{-1}, and three bands at 954, 941 and 926 cm^{-1} indicate six C–O–C bonds of glycosidic stretching modes (Lii, Stobinski, Tomasik, & Liao, 2003; Schuster, Ehmoser, Gapes, & Lendl, 2000; Zhang, 1994). In the Raman spectrum of the Chit-Amy-III derivative with an excitation wavelength of 785 nm (Fig. 5A-a), the band at 480 cm^{-1} is attributed to skeletal modes of pyranose rings of amylose (Fechner, Wartewig, Kleinebudde, & Neubert, 2005; Schuster et al., 2000). As expected, the α-1,4-glycosidic bonds of the Chit-Amy-III derivative appeared at 867 and 942 cm^{-1}. Furthermore, compared with the Raman spectra of the Chit-Glc7-IV and Chit-deg (Fig. 5A-b and A-c), more new bands of the Chit-Amy-III derivative appeared in the range from 950 to 1500 cm^{-1} (Fig. 5A-a), which are assigned to the glycosidic

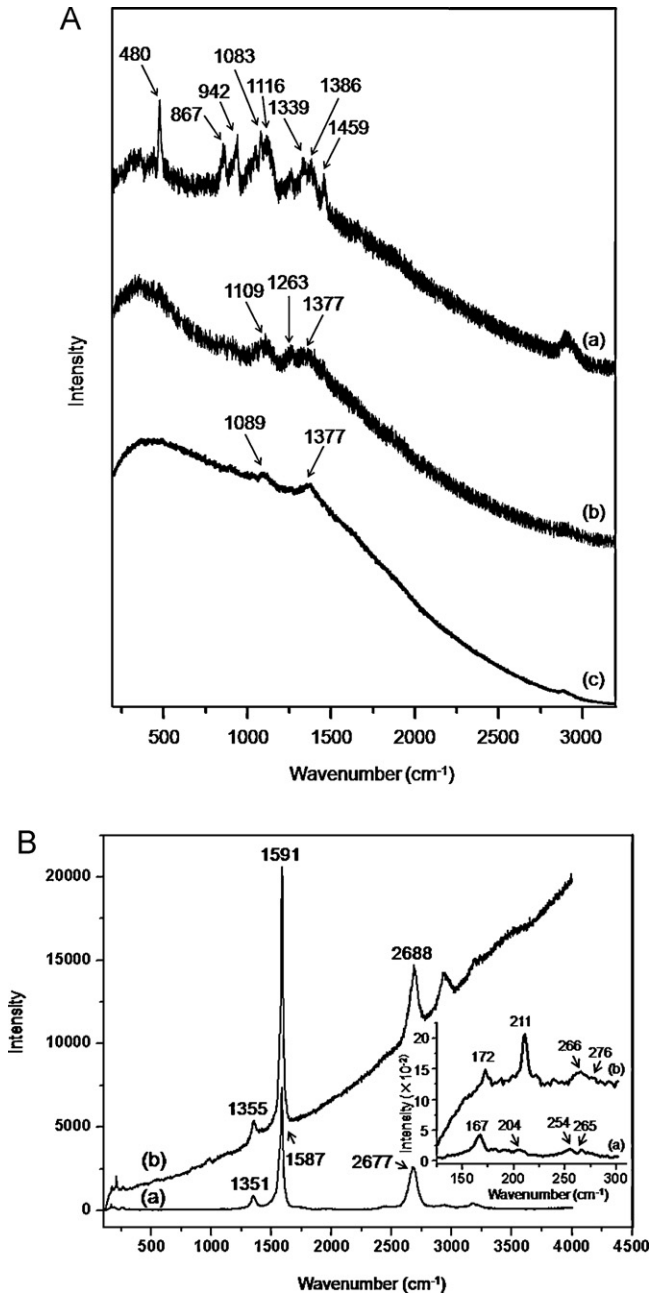

Fig. 5. Raman spectra of (A-a) Chit-Amy-III derivative, (A-b) Chit-Glc7-IV and (A-c) the Chit-deg excited at 785 nm, and (B-a) SWNTs and (B-b) Chit-Amy-SWNTs excited at 514.5 nm (insert: partly enlarged Raman spectra).

stretching modes and the CH_2 and C–OH deformations of amylose (Yang & Zhang, 2009). In view of the Raman results, the Chit-Amy-III is proved as an amylose-grafted chitosan derivative.

The XRD pattern of the Chit-Amy-III derivative shows the two diffraction peaks ($2\theta = 17.1^\circ$ and 22.1° in Fig. 4c), which is derived from the B-type structure of amylose with water uptake (Creek, Ziegler, & Runt, 2006; Potocki-Veronese et al., 2005). This further confirms the formation of amylose chains by phosphorylase-catalyzed enzymatic polymerization.

3.3. Formation and property of the Chit-Amy-SWNTs complex

The agglomeration and sedimentation of SWNTs occurred within 30 min in distilled water, even after ultrasonic dispersion (Fig. 6A-a). On the contrary, after the aqueous solution of the Chit-

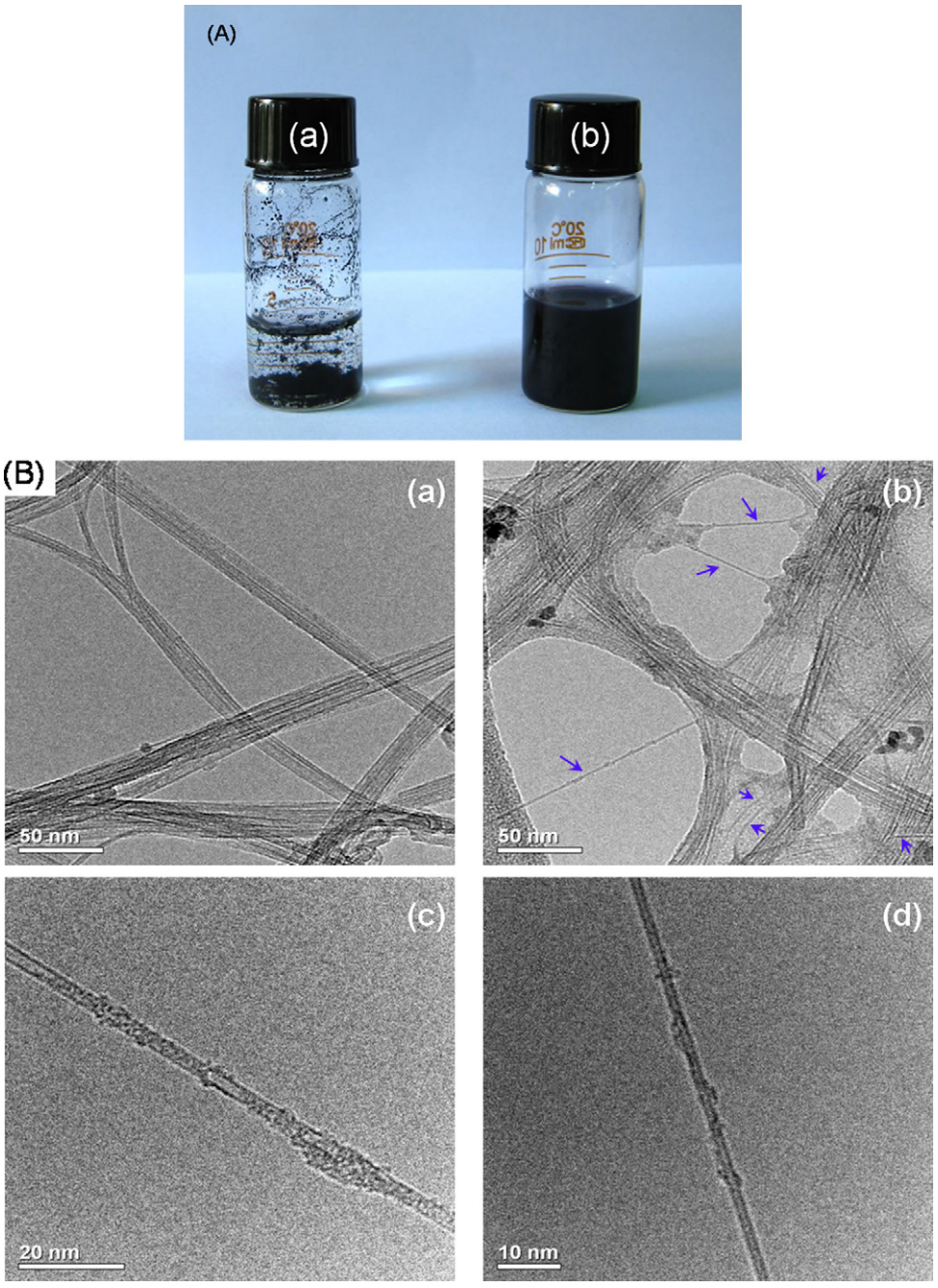

Fig. 6. (A) Photographs of (a) SWNTs, and (b) Chit-Amy-SWNTs, and (B) TEM images of (a) SWNTs, (b), (c) and (d) Chit-Amy-SWNTs.

Amy-III derivative and SWNTs underwent the ultrasonic treatment, a homogeneous black aqueous solution was obtained and no precipitation was observed upon prolonged standing for two weeks (Fig. 6A-b). The above observations have been confirmed by UV–vis spectrometry of the Chit-Amy-SWNTs complex (more information is available in Fig. S1 in the Supplementary Data).

Direct structural characterization of SWNTs before and after the complexation with the Chit-Amy-III derivative was realized by HR TEM imaging, and the images are presented in Fig. 6B. As expected, SWNTs are bundled into compact ropes (Fig. 6B-a). By the complexation with the Chit-Amy-III derivative, some SWNTs ropes are debundled into individual SWNTs (marked by arrows Fig. 6B-b). From the HR TEM images in Fig. 6B-c and B-d, it was further observed that the surface of the SWNTs is attached with the amorphous materials, which might be attributed to the wrapped Chit-Amy-III derivative at various sites.

The Raman spectra of the complex and SWNTs with an excitation wavelength of 514.5 nm are shown in Fig. 5B. The peak at about 1351 cm^{-1} is assigned to the disorder induced band (D-band) of SWNTs in Fig. 5B-a, arising from amorphous carbon particles and defects in SWNTs (Fu et al., 2007). In addition, a strong band located at about 1587 cm^{-1} are assigned to the graphite band (G-band), arising from sp^2-hybridised carbons atoms on the wall of SWNTs (Yang et al., 2008). About 4 cm^{-1} shift in the D-band and G-band can be observed in the spectrum of the Chit-Amy-SWNTs complex (Fig. 5B-b). Besides, it can be clearly seen that the peak of the D-band is still much smaller than that of the G-band, suggesting that the SWNTs have a perfect graphitic surface and even are not destroyed after being wrapped by the Chit-Amy-III derivative. For the SWNTs

sample, the radical breathing modes (RBMs) are mainly positioned at 167, 204, 254 and 265 cm^{-1} (curve 5B-a in insert). According to the inversely proportional relationship between RBM (ω_{RBM}) and the SWNTs diameter (d): $d = 224/(\omega_{RBM} - 14)$ (Rao et al., 2001), the observed peaks correspond to SWNTs with diameters of 1.5, 1.2, 0.93 and 0.89 nm. The RBM bands up-shift in the Raman spectrum of the Chit-Amy-SWNTs complex (curve 5B-b in insert). As the RBM band is sensitive to the perturbations in the local environment of SWNTs, the up-shift suggests a debundling process for the surface modification of SWNTs ropes (Chambers et al., 2003). This is probably caused as a result of non-covalent interactions between amylose chains of the Chit-Amy-III derivative and SWMTs according to the previous works (Chambers et al., 2003; Fu et al., 2007; Yang et al., 2008).

As shown in Fig. 4c–e, the XRD pattern of Chit-Amy-SWNTs complex is different from those of Chit-Amy-III derivative and SWNTs, in which three new diffraction peaks ($2\theta = 19.2^\circ$, 20.3° and 23.7°) appeared (Fig. 4d). They are attributed to the crystalline structure of helical inclusion complex of Chit-Amy-III derivative with SWNTs (inset in Fig. 4), matched with the XRD analysis of inclusion complex of amylose with poly(ε-caprolactone) (Kadokawa, Kaneko, Nakaya, & Tagaya, 2001; Kaneko & Kadokawa, 2005). Therefore, the XRD data further confirms the complexation of Chit-Amy-III derivative with SWNTs.

3.4. Electrochemical property of the Chit-Amy-SWNTs complex modified electrode

The detection of H_2O_2 is important because it is an essential mediator in biomedical and environmental industries (Lin, Tsai, & Chen, 2010; Tong, Yuan, Chai, Chen, & Xie, 2007). The high electron conductivity and electrocatalytic activity of nanotubes on H_2O_2 was reported in the previous works (Rubianes & Rivas, 2003; Yang, Yang, Yang, Shen, & Yu, 2006). Therefore, the electrochemical property of the Chit-Amy-SWNTs complex modified electrode was investigated using cyclic voltammetry and through the amperometric response to H_2O_2.

Fig. 7A compares the cyclic voltammograms recorded for naked and Chit-Amy-SWNTs complex modified GC electrodes in the background phosphate buffer solution (pH 7.0) (curves a and c) and in the electrolyte solution containing H_2O_2 (curves b and d). Both the background current and H_2O_2 redox current of the Chit-Amy-SWNTs modified electrode were stronger than those of the naked electrode. This confirmed that the Chit-Amy-SWNTs complex was successfully immobilized onto the electrode surface and showed good conductivity. For the Chit-Amy-SWNTs modified electrode, the stronger H_2O_2 redox current appeared following adding H_2O_2 in the electrolyte solution (curve d), suggesting the good electrocatalytic activity to H_2O_2.

The H_2O_2 redox current of the Chit-Amy-SWNTs modified electrode clearly increase with increasing potential scan rate as shown in Fig. 7B. The plot of anodic peak current (i) vs. the square root of the scan rate ($v^{1/2}$) from 100 to 400 mV/s showed a linear relation (inset in Fig. 7B), indicating a diffusion-controlled feature of the redox process of H_2O_2 at the modified electrode surface according to the literature (Yang et al., 2006).

The stability of the Chit-Amy-SWNTs modified electrode is a critical feature for its successful practical application, which was examined by cyclic voltammetry with 50 scans. The superposition of cyclic voltammetric voltammograms indicates good stability of the electrode (Fig. S2 in Supplementary Data).

Fig. 8 displays the amperometric response for the different electrodes following successive addition of H_2O_2 to the phosphate buffer solution (pH 7.0). Compared with the naked electrode and the Chit-Amy-III derivative modified electrode (Fig. 8b and c), faster and more sensitive response of the Chit-Amy-SWNTs com-

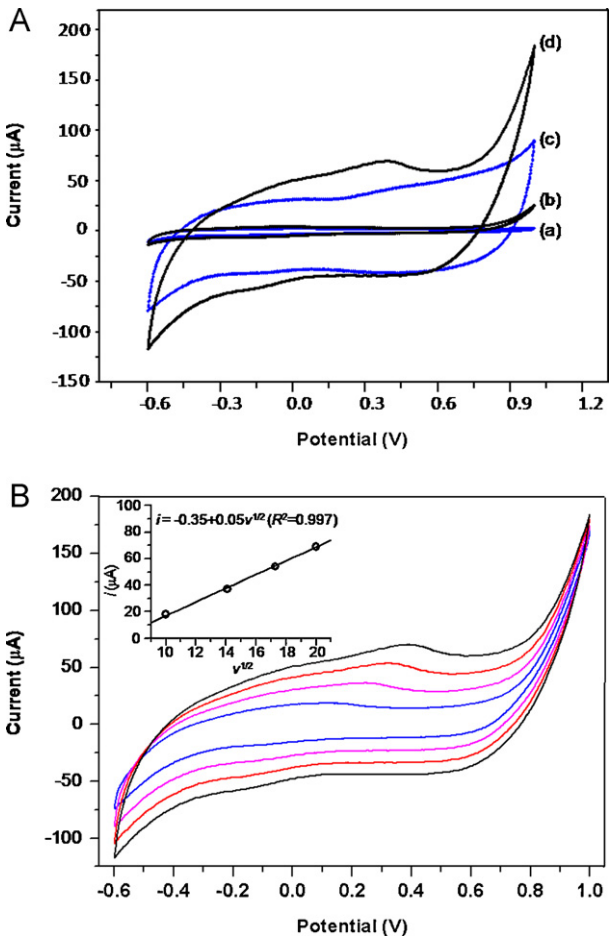

Fig. 7. (A) Cyclic voltammograms of (a) the naked electrode in the background phosphate buffer solution (pH 7.0), (b) the naked electrode in phosphate buffer solution (pH 7.0) containing 2 mmol/L H_2O_2, (c) the Chit-Amy-SWNTs complex modified electrode in the background phosphate buffer solution (pH 7.0), (d) the Chit-Amy-SWNTs complex modified electrode in phosphate buffer solution (pH 7.0) containing 2 mmol/L H_2O_2 with scan rate at 400 mV s^{-1}. (B) Voltammetric voltammograms of the Chit-Amy-SWNTs complex modified electrode in phosphate buffer solution (pH 7.0) containing 2 mmol/L H_2O_2 at different scan rates (v) (inner to outer): 100, 200, 300 and 400 mV s^{-1}. Inset: plot of anodic peak current (i) vs. $v^{1/2}$.

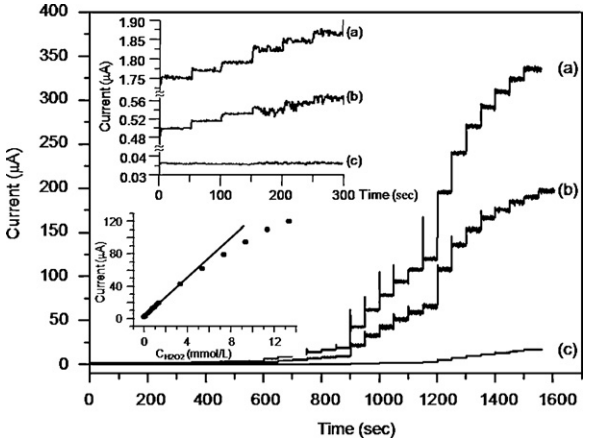

Fig. 8. The amperometric responses of (a) the Chit-Amy-SWNTs complex modified electrode, (b) the naked electrode, and (c) the Chit-Amy-III derivative modified electrode to successive addition of 0.001–8.8 mol/L H_2O_2 in phosphate buffer solution (pH 7.0) at an applied potential of 1.0 V. Inset: enlarged amperometric response, and calibration curve of current vs. H_2O_2 concentrations for the Chit-Amy-SWNTs complex modified electrode ($I = 2.0 \times 10^{-6} + 0.13C_{H_2O_2}$, $R^2 = 0.998$).

plex modified electrode was observed (Fig. 8a), of which the time required to reach the steady state response was about 1 s. This may be due to the good conductivity of SWNTs and the easy diffusion H_2O_2 in the Chit-Amy-SWNTs films. In contrast, the detectable respond of the Chit-Amy-III derivative modified electrode was weak (Fig. 8c), as a result of the non-conductivity of the Chit-Amy-III derivative. The calibration curve for detection H_2O_2 of the Chit-Amy-SWNTs complex modified electrode was shown in the inset of Fig. 8. The response was linear over the concentration range from 0.32 μmol/L to 33 mmol/L with a detection limit of 0.32 μmol/L. The result indicated that the Chit-Amy-SWNTs complex modified electrode displayed an acceptable performance to detect H_2O_2 and with broader linear range, similar to the DNA films modified H_2O_2 biosensors (Tong et al., 2007). The excellent electrocatalytic activity of the electrode toward H_2O_2 means that the Chit-Amy-SWNTs complex could be a promising candidate for future applications in biosensors, since H_2O_2 is a product of a large number of oxidase-based enzyme reactions (Chakraborty & Raj, 2009).

4. Conclusions

The water-soluble Chit-Glc7-IV and Chit-Amy-III derivatives were synthesized through the reductive amination and the phosphorylase-catalyzed enzymatic polymerization, respectively. The structures of maltoheptaose residues and short amylose chains grafted with chitosan backbones were confirmed by FTIR, ^1H NMR, Raman, XRD and static light scattering analyses. The dispersion stability of SWNTs in water could be improved through the Chit-Amy-SWNTs complex. Raman, XRD and TEM analyses proved that the complex was formed by the wrapping of the Chit-Amy-III derivative around the SWNTs. The result of electrochemical analysis indicated that the Chit-Amy-SWNTs complex modified electrode displayed excellent electron conductivity and electrocatalytic activity on H_2O_2.

Supplementary data available

Tables S1 and S2, scheme of synthesis of the Chit-Glc7 and Chit-Amy derivatives, UV–vis spectra of Chit-Amy-SWNTs complex and SWNTs, and ammetric voltammograms of the Chit-Amy-SWNTs complex modified electrode with different scan times are available free of charge via the Internet at http://www.elsevier.com.

Acknowledgements

This work was supported by the National Natural Science Foundation of China (20574089, 20974130), the Science and Technology Planning Project of Guangdong Province, China (2009B020313001), and the Fundamental Research Funds for the Central Universities, China (09lgpy14).

Appendix A. Supplementary data

Supplementary data associated with this article can be found, in the online version, at doi:10.1016/j.carbpol.2011.04.005.

References

Bhattarai, N., Edmondson, D., Veiseh, O., Matsen, F. A., & Zhang, M. (2005). Electrospun chitosan-based nanofibers and their cellular compatibility. *Biomaterials*, *26*, 6176–6184.

Braunmuhl, V., Jonas, G., & Stadler, R. (1995). Enzymatic grafting of amylose from poly(dimethylsi1oxanes). *Macromolecules*, *28*, 17–24.

Cesaro, A., Benegas, J. C., & Ripoll, D. R. (1986). Molecular model of the cooperative amylose–iodine–triiodide complex. *The Journal of Physical Chemistry*, *90*, 2787–2791.

Chambers, G., Carroll, C., Farrell, G. F., Dalton, A. B., McNamara, M., Panhuis, M., et al. (2003). Characterization of the interaction of gamma cyclodextrin with single-walled carbon nanotubes. *Nano Letters*, *3*, 843–846.

Chakraborty, S., & Raj, C. R. (2009). Pt nanoparticle-based highly sensitive platform for the enzyme-free amperometric sensing of H_2O_2. *Biosensors and Bioelectronics*, *24*, 3264–3268.

Cohen, R., Orlova, Y., Kovalev, M., Ungar, Y., & Shimoni, E. (2008). Structural and functional properties of amylose complexes with genistein. *Journal of Agricultural and Food Chemistry*, *56*, 4212–4218.

Creek, J. A., Ziegler, G. R., & Runt, J. (2006). An amylose crystallization from concentrated aqueous solution. *Biomacromolecules*, *7*, 761–770.

Cruz, D. M. G., Ivirico, J. L. E., Gomes, M. M., Ribelles, J. L. G., Sanchez, M. S., Reis, R. L., et al. (2008). Chitosan microparticles as injectable scaffolds for tissue engineering. *Journal of Tissue Engineering and Regenerative Medicine*, *2*, 378–380.

Ding, Y., Wang, Y., & Lei, Y. (2010). Direct electrochemistry and electrocatalysis of novel single-walled carbon nanotubes–hemoglobin composite microbelts-towards the development of sensitive and mediator-free biosensor. *Biosensors and Bioelectronics*, *26*, 390–397.

Fechner, P. M., Wartewig, S., Kleinebudde, P., & Neubert, R. H. H. (2005). Studies of the retrogradation process for various starch gels using Raman spectroscopy. *Carbohydrate Research*, *340*, 2563–2568.

Fu, C., Meng, L., Lu, Q., Zhang, X., & Gao, C. (2007). Large-scale production of homogeneous helical amylose/SWNTs complexes with good biocompatibility. *Macromolecular Rapid Communication*, *28*, 2180–2184.

Gelders, G. G., Goesaert, H., & Delcour, J. A. (2005). Potato phosphorylase catalyzed synthesis of amylose–lipid complexes. *Biomacromolecules*, *6*, 2622–2629.

Gidley, M. J., & Bulpin, P. V. (1989). Aggregation of amylose in aqueous systems: The effect of chain length on phase behavior and aggregation kinetics. *Macromolecules*, *22*, 341–346.

Gooding, J. J., Wibowo, R., Liu, J., Yang, W., Losic, D., Orbons, S., et al. (2003). Protein electrochemistry using aligned carbon nanotube arrays. *Journal of the American Chemical Society*, *125*, 9006–9007.

Gottlieb, H. E., Kotlyar, V., & Nudelman, A. (1997). NMR chemical shifts of common laboratory solvents as trace impurities. *The Journal of Organic Chemistry*, *62*, 7512–7515.

Heinemann, C., Escher, F., & Conde-Petit, B. (2003). Structural features of starch–lactone inclusion complexes in aqueous potato starch dispersions: The role of amylose and amylopectin. *Carbohydrate Polymers*, *51*, 159–168.

Izawa, H., Nawaji, M., Kaneko, Y., & Kadokawa, J. (2009). Preparation of glycogen-based polysaccharide materials by phosphorylase-catalyzed chain elongation of glycogen. *Macromolecular Bioscience*, *9*, 1098–1104.

Kadokawa, J., Kaneko, Y., Nakaya, A., & Tagaya, H. (2001). Formation of an amylose olyester inclusion complex by means of phosphorylase-catalyzed enzymatic polymerization of α-D-glucose 1-phosphate monomer in the presence of poly(ε-caprolactone). *Macromolecules*, *34*, 6536–6538.

Kaneko, Y., & Kadokawa, J. (2005). Vine-twining polymerization: A new preparation method for well-defined supramolecules composed of amylose and synthetic polymers. *The Chemical Record*, *5*, 36–46.

Kaneko, Y., Matsuda, S., & Kadokawa, J. (2007). Chemoenzymatic syntheses of amylose-grafted chitin and chitosan. *Biomacromolecules*, *8*, 3959–3964.

Kato, Y., Onishi, H., & Machida, Y. (2004). *N*-Succinyl-chitosan as a drug carrier: Water-insoluble and water-soluble conjugates. *Biomaterials*, *25*, 907–915.

Lalush, I., Bar, H., Zakaria, I., Eichler, S., & Shimoni, E. (2005). Utilization of amylose–lipid complexes as molecular nanocapsules for conjugated linoleic acid. *Biomacromolecules*, *6*, 121–130.

Lii, C., Stobinski, L., Tomasik, P., & Liao, C. (2003). Single-walled carbon nanotube—potato amylose complex. *Carbohydrate Polymers*, *51*, 93–98.

Lin, K. C., Tsai, T. H., & Chen, S. M. (2010). Performing enzyme-free H_2O_2 biosensor and simultaneous determination for AA, DA, and UA by MWCNT–PEDOT film. *Biosensors and Bioelectronics*, *26*, 608–614.

Loos, K., Braunmuh, V., & Stadler, R. (1997). Saccharide modified silica particles by enzymatic grafting. *Macromolecular Rapid Communication*, *18*, 927–938.

Lu, B., Wang, C., Wu, D., Li, C., Zhang, X., & Zhuo, R. (2009). Chitosan based oligoamine polymers: Synthesis, characterization, and gene delivery. *Journal of Controlled Release*, *137*, 54–62.

Martino, A, Sittinger, M., & Risbud, M. V. (2005). Chitosan: A versatile biopolymer for orthopaedic tissue-engineering. *Biomaterials*, *26*, 5983–5990.

Matsuda, S., Kaneko, Y., & Kadokawa, J. (2007). Chemoenzymatic synthesis of amylose-grafted chitosan. *Macromolecular Rapid Communication*, *28*, 863–867.

Najeeb, C. K., Chang, J., Lee, J. H., Lee, M., & Kim, J. H. (2011). Preparation of semiconductor-enriched single-walled carbon nanotube dispersion using a neutral pH water soluble chitosan derivative. *Journal of Colloid and Interface Science*, *354*, 461–466.

Nishimura, S. I., Kohgo, O., Kurita, K., & Kuzuhara, H. (1991). Chemospecific manipulations of a rigid polysaccharide: Syntheses of novel chitosan derivatives with excellent solubility in common organic solvents by regioselective chemical modifications. *Macromolecules*, *24*, 4745–4748.

Omagari, Y., Matsuda, S., Kaneko, Y., & Kadokawa, J. (2009). Chemoenzymatic synthesis of amylose-grafted cellulose. *Macromolecular Bioscience*, *9*, 450–455.

Omagari, Y., Kaneko, Y., & Kadokawa, J. (2010). Chemoenzymatic synthesis of amylose-grafted alginate and its formation of enzymatic disintegratable beads. *Carbohydrate Polymers*, *82*, 394–400.

Park, J. H., Cho, Y. W., Chung, H., Kwon, I. C., & Jeong, S. Y. (2003). Synthesis and characterization of sugar-bearing chitosan derivatives: Aqueous solubility and biodegradability. *Biomacromolecules*, *4*, 1087–1091.

Pfannemuller, B., Mayerhofer, H., & Schulz, R. C. (1971). Conformation of amylose in aqueous solution: Optical rotatory dispersion and circular dichroism of amylose–iodine complexes and dependence on chain length of retrogradation of amylose. *Biopolymers*, *10*, 243–261.

Potocki-Veronese, G., Putaux, J. L., Dupeyre, D., Albenne, C., Remaud-Simon, M., Monsan, P., et al. (2005). Amylose synthesized in vitro by amylosucrase: Morphology, structure, and properties. *Biomacromolecules*, *6*, 1000–1011.

Qin, C. Q., Du, Y. M., & Xiao, L. (2002). Effect of hydrogen peroxide treatment on the molecular weight and structure of chitosan. *Polymer Degradation and Stability*, *76*, 211–218.

Rao, A. M., Chen, J., Richter, E., Schlecht, U., Eklund, P. C., Haddon, R. C., et al. (2001). Effect of van derWaals interactions on the Raman modes in single walled carbon nanotubes. *Physical Review Letters*, *86*, 3895–3898.

Rubianes, M. D., & Rivas, G. A. (2003). Carbon nanotubes paste electrode. *Electrochemical Communication*, *5*, 689–694.

Schuster, K. C., Ehmoser, H., Gapes, J. R., & Lendl, B. (2000). On-line FT-Raman spectroscopic monitoring of starch gelatinisation and enzyme catalysed starch hydrolysis. *Vibrational Spectroscopy*, *22*, 181–190.

Shi, L., Liu, X., Niu, W., Li, H., Han, S., Chen, J., et al. (2009). Hydrogen peroxide biosensor based on direct electrochemistry of soybean peroxidase immobilized on single-walled carbon nanohorn modified electrode. *Biosensors and Bioelectronics*, *24*, 1159–1163.

Star, A., Steuerman, D. W., Heath, J. R., & Stoddart, J. F. (2002). Starched carbon nanotubes. *Angewandte Chemie International Edition*, *41*, 2508–2512.

Strand, S. P., Issa, M. M., Christensen, B. E., Varum, K. M., & Artursson, P. (2008). Tailoring of chitosans for gene delivery: Novel self-branched glycosylated chitosan oligomers with improved functional properties. *Biomacromolecules*, *9*, 3268–3276.

Tong, Z., Yuan, R., Chai, Y., Chen, S., & Xie, Y. (2007). Direct electrochemistry of horseradish peroxidase immobilized on DNA/electrodeposited zirconium dioxide modified, gold disk electrode. *Biotechnology Letters*, *29*, 791–795.

Wang, A. (2008). *Chitin chemistry* (1st ed.). Beijing: Science Press., pp. 169–200, 147–148, 181

Wang, W., Bo, S., & Qin, W. (1991). Determination of the Mark–Houwink equation for chitosans with different degrees of deacetylation. *International Journal of Biological Macromolecules*, *13*, 281–285.

Wu, J. (1994). *Techniques and application of modern FTIR spectroscopy*. Beijing: Science and Technology Press., pp. 603.

Yang, M., Yang, Y., Yang, H., Shen, G., & Yu, R. (2006). Layer-by-layer self-assembled multilayer films of carbon nanotubes and platinum nanoparticles with polyelectrolyte for the fabrication of biosensors. *Biomaterials*, *27*, 246–255.

Yang, L., Zhang, B., Liang, Y., Yang, B., Kong, T., & Zhang, L. (2008). In situ synthesis of amylose/single-walled carbon nanotubes supramolecular assembly. *Carbohydrate Research*, *343*, 2463–2467.

Yang, L., & Zhang, L. (2009). Chemical structural and chain conformational characterization of some bioactive polysaccharides isolated from natural sources. *Carbohydrate Polymers*, *76*, 349–361.

Yu, J., Li, Y., Qiu, L., & Jin, Y. (2008). Self-aggregated nanoparticles of cholesterol-modified glycol chitosan conjugate: Preparation, characterization, and preliminary assessment as a new drug delivery carrier. *European Polymer Journal*, *44*, 555–565.

Zhang, M., Smith, A., & Gorski, W. (2004). Carbon nanotube chitosan system for electrochemical sensing based on dehydrogenase enzyme. *Analytical Chemistry*, *76*, 5045–5050.

Zhang, W. (1994). *Biochemical technology of carbohydrate complexes*. Hangzhou: Zhejiang University Press., pp. 193–200.

Ziegast, G., & Pfannemuller, B. (1987). Phosphorolytic syntheses with di-, oligo- and multi-functional primers. *Carbohydrate Research*, *160*, 185–204.